Available online at www.sciencedirect.com
SCIENCE DIRECT®
Journal of Sound and Vibration 276 (2004) 245–271
JOURNAL OF SOUND AND VIBRATION
www.elsevier.com/locate/jsvi

Spatial free vibration of shear deformable circular curved beams with non-symmetric thin-walled sections

Nam-Il Kim, Moon-Young Kim*

Department of Civil and Environmental Engineering, Sungkyunkwan University, Cheoncheon-Dong, Jangan-Ku, Suwon 440-746, South Korea

Received 19 December 2002; accepted 25 July 2003

Abstract

For spatial free vibration of *shear deformable* circular curved beams with non-symmetric thin-walled cross-sections, an improved vibration theory is proposed. The elastic strain and kinetic energies are first derived by considering constant curvature effects and shear deformation effects due to shear forces and restrained warping torsion. Next equilibrium equations and force–deformation relations are obtained using a stationary condition of total potential energy. And then the closed-form solution for out-of-plane vibration of curved beam is newly derived. In addition F. E. procedures are developed by using isoparametric curved beam element with arbitrary thin-walled sections. In order to illustrate the accuracy and the practical usefulness of this study, closed-form and numerical solutions for spatial free vibration are compared with results by available references and ABAQUS's shell element. Particularly not only shear deformation and thickness–curvature effects on vibration behaviors of curved beams but also *mode transition* and crossover phenomena with change in curvatures and the length of beams are parametrically investigated.

1. Introduction

The spatially vibrational behavior of thin-walled curved beam structures is very complex due to the coupling effect of extensional, bending and torsional deformation. Investigation into the free vibration for thin-walled curved members with open and closed cross-sections has been carried out extensively since the early works of Vlasov [1] and Timoshenko and Gere [2].

Many researches [3–21] on the free in-plane vibration of curved beam have been done considering various parameters such as boundary conditions, shear deformation, rotary inertia,

*Corresponding author. Tel.: +82-31-290-7514; fax: +82-31-290-7548.
E-mail address: kmye@skku.ac.kr (M.-Y. Kim).

0022-460X/$ - see front matter
doi:10.1016/j.jsv.2003.07.036

variable curvatures and variable cross-sections. Particularly several authors [3–13] have reported on the *mode transition phenomena* which are characterized by sharp increase in frequencies of some modes that occurs at combinations of curvature and length of curved beam. Tarnopolskaya et al. [3,4] examined the phenomenon of mode transition from extensional to inextensional that accompanies an increase in beam curvature. Chidamparam and Leissa [5] investigated the influence of extensibility on the in-plane free vibration frequencies of loaded circular arches and the crossover phenomenon which occur at the crossings of the frequency curves under the extensional condition. Also Charpie and Burroughs [6] presented an analytical model for the free in-plane vibration of curved beam with variable curvature and depth and concluded that the vibration frequencies and mode shapes are far more dependent upon variable depth than upon curvature. Scott and Woodhouse [7] studied the vibration of S-shaped strip of uniform cross-section and interpreted the variation of frequency with change in curvature by membrane and bending theories. Petyt and Fleischer [8] examined the transformation of the mode shape at the stage of the increase in eigenvalues using the finite-element analysis. Even though a significant amount of research has been conducted on the frequency crossover phenomenon for the vibration of curved beam, it is judged that most of these studies was limited to only the in-plane free vibration behavior and did not analyze the effect of shear deformation in connection with frequency crossover.

On the other hand, the research for spatial free vibrations including the out-of-plane vibration behavior of curved beam has been performed by several authors [22–34]. Cortinez et al. [22] and Piovan et al. [23] investigated the out-of-plane vibration of simply and continuous supported thin-walled curved beam with shear deformation but they did not take fully into account the effect of thickness-curvature and shear deformation due to shear forces and restrained torsional moment of curved beam. Interestingly for the spatially coupled vibrational behavior of curved beam, Gendy and Saleeb [33] presented an effective formulation on spatial free vibration of arbitrary thin-walled curved beam by including the shear deformation and rotary inertia. However, they partially considered the effect of thickness-curvature and shear deformation. Recently Kim et al. [34] presented an analytical and numerical solutions on a spatial free vibration of thin-walled curved beam with non-symmetric section neglecting shear deformation effects.

Despite those extensive studies, it is judged that there still remain some margins to improve in formulating coupled vibration problems of curved beams having non-symmetric thin-walled cross-sections. Namely, it is necessary to present an improved formulation taking into account (1) *non-symmetry* of thin-walled cross-sections, (2) the so-called *thickness-curvature effects*, and (3) *shear deformation effects* due to shear forces and warping-torsion. Also, one needs to derive (4) *closed-form solutions* for out-of-plane vibration modes of monosymmetric circular beams and to perform (5) the *parametric study* on spatially free vibration behaviors of curved beams.

Accordingly the primary aim of this study is to present an improved formulation for spatial free vibration analysis of shear deformable curved beams having arbitrary thin-walled cross-sections, to newly derive the closed-form solution for monosymmetric circular beams, and to present the parametric study for vibrational behaviors of curved beams. The important points presented are summarized as follows:

1. The *shear deformable* displacement field for *non-symmetric* thin-walled curved beams having constant curvatures is first introduced in which all parameters including the normalized warping function are defined at the centroid.

2. Next force–deformation relationships due to simple shear and *warping-torsional shear* stresses as well as normal stresses considering the thickness-curvature effects are presented in the general form.
3. And then the elastic strain and kinetic energies of curved beams considering shear deformation effects due to shear forces and warping-torsion are formulated and the resulting equilibrium equations of curved beams are derived using the stationary principle of the total potential energy.
4. Closed-form solutions are newly derived for out-of-plane free vibration of monosymmetric thin-walled curved beams and also, F.E. procedures are presented by developing isoparametric curved beam elements with arbitrary thin-walled sections.
5. Finally spatial free vibration behavior of curved beams is investigated through the parametric studies. Particularly, not only shear deformation and thickness-curvature effects but also *mode transition* and crossover phenomena with change in curvature are investigated on spatial free vibration for non-symmetric curved beams.

2. A spatial free vibrational theory of shear deformable thin-walled curved beams

To degenerate a spatial free vibrational theory for the continuum to that for the thin-walled curved beam, the following assumptions are adopted:

1. The thin-walled curved beam is linearly elastic and prismatic.
2. The cross-section of the thin-walled curved beam is not deformed in its own plane. Accordingly, the effects of distortional deformations are negligible.
3. The axis of curvature does not necessarily coincide with one of the principal axes.
4. Shear deformations due to shear forces and restrained warping torsion are taken into account.

It is worth remarking that actually the contour of curved beams with unstiffened closed cross-sections deforms substantially more than open ones when warping effects are present. Therefore, the validity of the second assumption requires that the cross-section is fairly thick or adequately stiffened by its own plane rigid diaphragms. Nevertheless, as a practical matter, bulkheads or frames are usually present; then there is a large field of application of this simplified theory [35]. Referring to the fourth assumption, plane sections originally normal to the centroid axis remain plane and undistorted under deformation but not necessarily normal to this axis. Consequently, the warping modes remain unchanged in evaluating the shear strain energy due to bending-shear and warping-shear stresses.

2.1. Kinematics and force–deformation relations of thin-walled curved beams

To develop a general theory for free vibration analysis of *shear deformable* thin-walled curved beams consistently, a curvilinear co-ordinate system (x_1, x_2, x_3) shown in Fig. 1 is adopted in which the x_1-axis coincides with a centroid axis having the radius of curvature R but x_2, x_3 are not necessarily principal inertia axes according to assumption 3. In this study, the phrases "in-plane" and "out-of-plane" are frequently used, which are referred to x_1–x_3 plane (the plane of curvature) and x_1–x_2 plane, respectively.

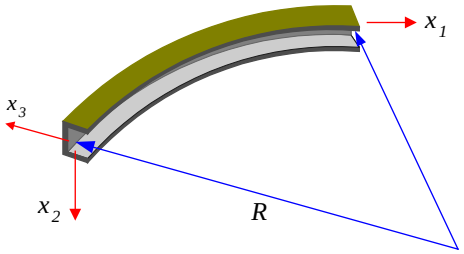

Fig. 1. Co-ordinate system of non-symmetric thin-walled curved beam.

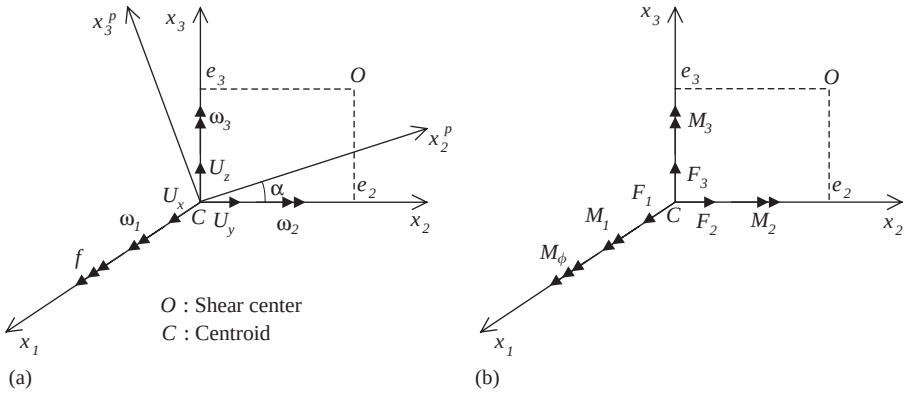

Fig. 2. Notation for (a) displacement parameters and (b) stress resultants.

Now to introduce the displacement field for the non-symmetric thin-walled cross-section, seven displacement parameters are shown in Fig. 2(a). U_x, U_y, U_z and $\omega_1, \omega_2, \omega_3$ are rigid body translations and rotations of the cross-section with respect to x_1, x_2 and x_3 axes, respectively. f is a displacement parameter measuring warping deformations. In addition, (x_2^p, x_3^p) means principal axes defined at the centroid where α is the angle between x_2^p and x_2 axes in the counterclockwise direction. Assuming that the cross-section is rigid in its own plane, the total displacement field can be written as follows:

$$U_1 = U_x - x_2\omega_3 + x_3\omega_2 + f\phi(x_2, x_3), \tag{1a}$$

$$U_2 = U_y - x_3\omega_1, \tag{1b}$$

$$U_3 = U_z + x_2\omega_1, \tag{1c}$$

where ϕ is the normalized warping function defined at the centroid.

An improved stability theory including force–deformation relations of shear deformable curved beams having non-symmetric thin-walled cross-sections have been already derived in the study of

Kim et al. [36]. Hence, force–deformation relations that need to develop a vibrational formulation of curved beams are shortly summarized and then the kinetic energy is newly derived. Stress resultants with respect to the centroid are defined as follows:

$$F_1 = \int_A \tau_{11}\,\mathrm{d}A, \quad F_2 = \int_A \tau_{12}\,\mathrm{d}A, \quad F_3 = \int_A \tau_{13}\,\mathrm{d}A, \quad M_1 = \int_A (\tau_{13}x_2 - \tau_{12}x_3)\,\mathrm{d}A,$$
$$M_2 = \int_A \tau_{11}x_3\,\mathrm{d}A, \quad M_3 = -\int_A \tau_{11}x_2\,\mathrm{d}A, \quad M_\phi = \int_A \tau_{11}\phi\,\mathrm{d}A,$$
$$M_R = \int_A \left[\tau_{12}\phi_{,2} + \tau_{13}\left(\phi_{,3} - \frac{\phi}{R+x_3}\right)\right]\frac{R+x_3}{R}\,\mathrm{d}A, \tag{2a–h}$$

where F_1 is the axial force, F_2 and F_3 are the shear forces acting at the centroid, M_1 the total twist moment with respect to the centroid axis, M_2 and M_3 are the bending moments with respect to x_2 and x_3 axes, M_R and M_ϕ are the restrained torsional moment and the bimoment about the x_1 axis. In addition, sectional properties are defined by

$$I_2 = \int_A x_3^2\,\mathrm{d}A, \quad I_3 = \int_A x_2^2\,\mathrm{d}A, \quad I_{23} = \int_A x_2x_3\,\mathrm{d}A, \quad I_\phi = \int_A \phi^2\,\mathrm{d}A,$$
$$I_{\phi 2} = \int_A \phi x_3\,\mathrm{d}A, \quad I_{\phi 3} = \int_A \phi x_2\,\mathrm{d}A, \quad I_{222} = \int_A x_3^3\,\mathrm{d}A, \quad I_{223} = \int_A x_2x_3^2\,\mathrm{d}A,$$
$$I_{233} = \int_A x_2^2x_3\,\mathrm{d}A, \quad I_{333} = \int_A x_2^3\,\mathrm{d}A, \quad I_{\phi 22} = \int_A \phi x_3^2\,\mathrm{d}A, \quad I_{\phi 33} = \int_A \phi x_2^2\,\mathrm{d}A,$$
$$I_{\phi 23} = \int_A \phi x_3x_2\,\mathrm{d}A, \quad I_{\phi\phi 2} = \int_A \phi^2x_3\,\mathrm{d}A, \quad I_{\phi\phi 3} = \int_A \phi^2x_2\,\mathrm{d}A, \tag{3a–o}$$

where A, I_2, I_3 and I_{23} are the cross-sectional area, second moments of inertia and product moment of inertia about x_2 and x_3 axes, respectively, I_ϕ the warping moment of inertia. Also, normal and shear strain–displacement relations may be expressed as follows:

$$e_{11} = \left[\left(U_x' + \frac{U_z}{R}\right) - x_2\left(\omega_3' - \frac{\omega_1}{R}\right) + x_3\omega_2' + \phi f'\right]\frac{R}{R+x_3}, \tag{4a}$$

$$2e_{12} = (U_y' - \omega_3)\frac{R}{R+x_3} - \left(\phi_{,2} + \frac{x_3R}{R+x_3}\right)\left(\omega_1' + \frac{\omega_3}{R}\right) + \left(f + \omega_1' + \frac{\omega_3}{R}\right)\phi_{,2}, \tag{4b}$$

$$2e_{13} = \left(U_z' + \omega_2 - \frac{U_x}{R}\right)\frac{R}{R+x_3} + \left(\frac{x_2R}{R+x_3} - \phi_{,3} + \frac{\phi}{R+x_3}\right)\left(\omega_1' + \frac{\omega_3}{R}\right)$$
$$+ \left(f + \omega_1' + \frac{\omega_3}{R}\right)\left(\phi_{,3} - \frac{\phi}{R+x_3}\right). \tag{4c}$$

Now substituting Eq. (4a) into Eqs. (2a), (2e)–(2g) and integrating over the cross-section leads to

$$\begin{pmatrix} F_1 \\ M_2 \\ M_3 \\ M_\phi \end{pmatrix} = E \begin{bmatrix} A + \dfrac{\hat{I}_2}{R^2} & -\dfrac{\hat{I}_2}{R} & \dfrac{\hat{I}_{23}}{R} & -\dfrac{\hat{I}_{\phi 2}}{R} \\ -\dfrac{\hat{I}_2}{R} & \hat{I}_2 & -\hat{I}_{23} & \hat{I}_{\phi 2} \\ \dfrac{\hat{I}_{23}}{R} & -\hat{I}_{23} & \hat{I}_3 & -\hat{I}_{\phi 3} \\ -\dfrac{\hat{I}_{\phi 2}}{R^2} & \hat{I}_{\phi 2} & -\hat{I}_{\phi 3} & \hat{I}_\phi \end{bmatrix} \begin{pmatrix} U_x' + \dfrac{U_z}{R} \\ \omega_2' \\ \omega_3' - \dfrac{\omega_1}{R} \\ f' \end{pmatrix}, \tag{5a–d}$$

where E is the Young modulus and

$$\hat{I}_2 = I_2 - \frac{I_{222}}{R}, \quad \hat{I}_3 = I_3 - \frac{I_{233}}{R}, \quad \hat{I}_{23} = I_{23} - \frac{I_{223}}{R},$$
$$\hat{I}_\phi = I_\phi - \frac{I_{\phi\phi 2}}{R}, \quad \hat{I}_{\phi 3} = I_{\phi 3} - \frac{I_{\phi 23}}{R}, \quad \hat{I}_{\phi 2} = I_{\phi 2} - \frac{I_{\phi 22}}{R} \tag{6a–f}$$

and also, the following approximation is used:

$$\frac{R}{R + x_3} \cong 1 - \frac{x_3}{R} + \left(\frac{x_3}{R}\right)^2. \tag{7}$$

On the other hand, it may be assumed that the force–deformation relations for shear forces, restrained torsional moment and St. Venant torsion in *curved* beams take the same form as those in *straight* beams [37] except that the curvature effect terms should be added to average shear deformations. Accordingly force–deformation relations due to shear stresses are given by

$$\begin{pmatrix} F_2 \\ F_3 \\ M_R \end{pmatrix} = G \begin{bmatrix} A_2 & A_{23} & A_{2r} \\ A_{23} & A_3 & A_{3r} \\ A_{2r} & A_{3r} & A_r \end{bmatrix} \begin{pmatrix} U_y' - \omega_3 \\ U_z' - \dfrac{U_x}{R} + \omega_2 \\ \omega_1' + \dfrac{\omega_3}{R} + f \end{pmatrix}, \tag{8a–c}$$

$$M_{st} = M_1 - M_R = M_1 - M_\phi' = GJ\left(\omega_1' + \frac{\omega_3}{R}\right), \tag{8d}$$

where G is the shear modulus, J the torsional constant and

$$A_2 = A_2^s \cos^2\alpha + A_3^s \sin^2\alpha, \quad A_3 = A_3^s \cos^2\alpha + A_2^s \sin^2\alpha,$$
$$A_r = A_r^s + A_2^s e_3^2 + A_3^s e_2^2, \quad A_{23} = (A_2^s + A_3^s)\cos\alpha \sin\alpha,$$
$$A_{2r} = -A_2^s e_3 \cos\alpha - A_3^s e_2 \sin\alpha, \quad A_{3r} = -A_2^s e_3 \sin\alpha + A_3^s e_2 \cos\alpha, \tag{9a–f}$$

where A_2^s, A_3^s and A_r^s are the effective shear areas defined by

$$\frac{1}{A_2^s} = \frac{1}{I_{3p}^2}\int_A Q_3^2 \frac{\mathrm{d}s}{t}, \quad \frac{1}{A_3^s} = \frac{1}{I_{2p}^2}\int_A Q_2^2 \frac{\mathrm{d}s}{t}, \quad \frac{1}{A_r^s} = \frac{1}{(I_\phi^s)^2}\int_A Q_r^2 \frac{\mathrm{d}s}{t} \tag{10a–c}$$

and

$$I_{2p} = \int_A (x_3^p)^2 \, \mathrm{d}A, \quad I_{3p} = \int_A (x_2^p)^2 \, \mathrm{d}A, \quad I_\phi^s = \int_A (\phi^s)^2 \, \mathrm{d}A,$$
$$Q_2 = \int_0^s x_3^p t \, \mathrm{d}s, \quad Q_3 = \int_0^s x_2^p t \, \mathrm{d}s, \quad Q_r = \int_0^s \phi^s t \, \mathrm{d}s. \tag{11a–f}$$

Consequently Eqs. (5) and (8) constitute force–deformation relations of shear deformable thin-walled curved beams. In reference to Eq. (8d), it may be demonstrated that a supplementary equilibrium equation ($M_R = M_\phi'$) is satisfied between the bimoment M_ϕ and the restrained warping torsion M_R.

2.2. Principle of linearized virtual work for thin-walled curved beams

The principle of linearized virtual work for the general continuum vibrating harmonically is expressed as

$$\int_V \tau_{ij} \delta e_{ij} \, \mathrm{d}V - \omega^2 \int_V \rho U_i \delta U_i \, \mathrm{d}V = \int_S T_i \delta U_i \, \mathrm{d}S, \tag{12}$$

where τ_{ij} and e_{ij} are the stress and linear strain, respectively, ρ the density, ω the circular frequency, T_i the surface force, U_i the displacement.

In case of the thin-walled circular beam, Eq. (12) may be transformed to principle of the total potential energy Π as follows:

$$\Pi = \Pi_E - \Pi_M - \Pi_{ext}, \tag{13}$$

where the detailed expressions for each term of Π are

$$\Pi_E = \frac{1}{2} \int_0^L \int_A [\tau_{11} e_{11} + 2\tau_{12} e_{12} + 2\tau_{13} e_{13}] \frac{R + x_3}{R} \, \mathrm{d}A \, \mathrm{d}x_1, \tag{14a}$$

$$\Pi_M = \tfrac{1}{2} \rho \omega^2 \int_0^L \int_A [U_1^2 + U_2^2 + U_3^2] \frac{R + x_3}{R} \, \mathrm{d}A \, \mathrm{d}x_1, \tag{14b}$$

$$\Pi_{ext} = \frac{1}{2} \int_S T_i U_i \, \mathrm{d}S. \tag{14c}$$

Substituting the linear strain (4) into Eq. (14a) and integrating over the cross-sectional area, Eq. (14a) are reduced to the following equation:

$$\Pi_E = \frac{1}{2} \int_0^L \left[F_1 \left(U_x' + \frac{U_z}{R} \right) + M_2 \omega_2' + M_3 \left(\omega_3' - \frac{\omega_1}{R} \right) + M_\phi f' + F_2 (U_y' - \omega_3) \right.$$
$$\left. + F_3 \left(U_z' - \frac{U_x}{R} + \omega_2 \right) + (M_1 - M_R) \left(\omega_1' + \frac{\omega_3}{R} \right) + M_R \left(\omega_1' + \frac{\omega_3}{R} + f \right) \right] \mathrm{d}x_1. \tag{15}$$

Now substitution of the force–deformation relations (5) and (8) into Eq. (15) leads to the elastic strain energy:

$$\begin{aligned}\Pi_E = \frac{1}{2}\int_0^L \Bigg[& EA\left(U_x' + \frac{U_z}{R}\right)^2 + E\hat{I}_2\left(\omega_2' - \frac{U_x'}{R} - \frac{U_z}{R^2}\right)^2 + E\hat{I}_3\left(\omega_3' - \frac{\omega_1}{R}\right)^2 + E\hat{I}_\phi f'^2 \\ & + 2E\hat{I}_{\phi 2}\left(\omega_2' - \frac{U_x'}{R} - \frac{U_z}{R^2}\right)f' - 2E\hat{I}_{\phi 3}\left(\omega_3' - \frac{\omega_1}{R}\right)f' - 2E\hat{I}_{23}\left(\omega_3' - \frac{\omega_1}{R}\right)\left(\omega_2' - \frac{U_x'}{R} - \frac{U_z}{R^2}\right) \\ & + GJ\left(\omega_1' + \frac{\omega_3}{R}\right)^2 + GA_2(U_y' - \omega_3)^2 + GA_3\left(U_z' - \frac{U_x}{R} + \omega_2\right)^2 + GA_r\left(\omega_1' + \frac{\omega_3}{R} + f\right)^2 \\ & + 2GA_{23}(U_y' - \omega_3)\left(U_z' - \frac{U_x}{R} + \omega_2\right) + 2GA_{2r}(U_y' - \omega_3)\left(\omega_1' + \frac{\omega_3}{R} + f\right) \\ & + 2GA_{3r}\left(U_z' - \frac{U_x}{R} + \omega_2\right)\left(\omega_1' + \frac{\omega_3}{R} + f\right)\Bigg]\,\mathrm{d}x_1. \end{aligned} \tag{16}$$

Also substituting the displacement field (1) into Eq. (14b), the kinetic energy Π_M including shear deformation and rotary inertia can be obtained as

$$\begin{aligned}\Pi_M = \tfrac{1}{2}\rho\omega^2\int_0^L \Bigg[& A(U_x^2 + U_y^2 + U_z^2) + \tilde{I}_0\omega_1^2 + \tilde{I}_2\omega_2^2 + \tilde{I}_3\omega_3^2 + \tilde{I}_\phi f^2 + 2\frac{I_2}{R}(U_x\omega_2 - U_y\omega_1) \\ & - 2\frac{I_{23}}{R}(U_x\omega_3 - U_z\omega_1) - 2\tilde{I}_{23}\omega_2\omega_3 + 2\tilde{I}_{\phi 2}\omega_2 f - 2\tilde{I}_{\phi 3}\omega_3 f + 2\frac{I_{\phi 2}}{R}U_x f\Bigg]\,\mathrm{d}x_1, \end{aligned} \tag{17}$$

where

$$\begin{aligned} & \tilde{I}_0 = I_2 + I_3 + \frac{I_{222} + I_{233}}{R}, \quad \tilde{I}_2 = I_2 + \frac{I_{222}}{R}, \quad \tilde{I}_3 = I_3 + \frac{I_{233}}{R}, \quad \tilde{I}_{23} = I_{23} + \frac{I_{223}}{R} \\ & \tilde{I}_\phi = I_\phi + \frac{I_{\phi\phi 2}}{R}, \quad \tilde{I}_{\phi 2} = I_{\phi 2} + \frac{I_{\phi 22}}{R}, \quad \tilde{I}_{\phi 3} = I_{\phi 3} + \frac{I_{\phi 23}}{R}. \end{aligned} \tag{18a–g}$$

Finally invoking the stationary condition of the total potential energy, equations of motion and boundary conditions for curved beams are obtained as described in Appendix A.

In neglecting the shear deformations and putting θ in place of ω_1, Eqs. (16) and (17) are reduced and given in Appendix B, which are identical to Eqs. (10) and (12) in Kim et al. [34].

3. Closed-form solutions for monosymmetric thin-walled curved beams

We consider out-of-plane free vibration of thin-walled curved beams with the cross-section monosymmetric for the x_3 axis. In this case, it turns out that the section properties $(I_{23}, I_{223}, I_{333}, I_{\phi 2}, I_{\phi 22}, A_{23}, A_{3r})$ and initial stress resultants vanish so that in-plane and out-of-plane modes are decoupled. Consequently the potential energy Π_{out} corresponding to out-of-plane

vibrational mode is given as follows:

$$\Pi_{out} = \frac{1}{2}\int_0^L \left[E\hat{I}_3\left(\omega_3' - \frac{\omega_1}{R}\right)^2 + E\hat{I}_\phi f'^2 - 2E\hat{I}_{\phi 3}\left(\omega_3' - \frac{\omega_1}{R}\right)f' + GJ\left(\omega_1' + \frac{\omega_3}{R}\right)^2 + GA_2(U_y' - \omega_3)^2 + GA_r\left(\omega_1' + \frac{\omega_3}{R} + f\right)^2 + 2GA_{2r}(U_y' - \omega_3)\left(\omega_1' + \frac{\omega_3}{R} + f\right) - \rho\omega^2\{AU_y^2 + \tilde{I}_0\omega_1^2 + \tilde{I}_3\omega_3^2 + \tilde{I}_\phi f^2 - 2\frac{I_2}{R}U_y\omega_1 - 2\tilde{I}_{\phi 3}\omega_3 f\}\right] \mathrm{d}x_1. \tag{19}$$

From the stationary condition, governing equations and boundary conditions at $x_1 = 0, L$ are obtained as follows:

$$-GA_2(U_y'' - \omega_3') \underline{- GA_{2r}\left(\omega_1'' + \frac{\omega_3'}{R} + f'\right)} - \rho\omega^2\left(AU_y \underline{- \frac{I_2}{R}\omega_1}\right) = 0, \tag{20a}$$

$$\underline{-\frac{E\hat{I}_3}{R}\left(\omega_3' - \frac{\omega_1}{R}\right) + \frac{E\hat{I}_{\phi 3}}{R}f'} - GJ\left(\omega_1'' + \frac{\omega_3'}{R}\right) - GA_r\left(\omega_1'' + \frac{\omega_3'}{R} + f'\right) \underline{- GA_{2r}(U_y'' - \omega_3')} - \rho\omega^2\left(\tilde{I}_0\omega_1 \underline{- \frac{I_2}{R}U_y}\right) = 0, \tag{20b}$$

$$-E\hat{I}_3\left(\omega_3'' - \frac{\omega_1'}{R}\right) + E\hat{I}_{\phi 3}f'' + \frac{GI}{R}\left(\omega_1' + \frac{\omega_3}{R}\right) - GA_2(U_y' - \omega_3) \underline{+ \frac{GA_r}{R}\left(\omega_1' + \frac{\omega_3}{R} + f\right) + GA_{2r}\left\{\frac{U_y' - \omega_3}{R} - \left(\omega_1' + \frac{\omega_3}{R} + f\right)\right\}} - \rho\omega^2(\tilde{I}_3\omega_3 - \tilde{I}_{\phi 3}f) = 0, \tag{20c}$$

$$\underline{-E\hat{I}_\phi f'' + E\hat{I}_{\phi 3}\left(\omega_3'' - \frac{\omega_1'}{R}\right)} + GA_r\left(\omega_1' + \frac{\omega_3}{R} + f\right) \underline{+ GA_{2r}(U_y' - \omega_3)} - \rho\omega^2(\tilde{I}_\phi f \underline{- \tilde{I}_{\phi 3}\omega_3}) = 0 \tag{20d}$$

and

$$\delta U_y = 0 \quad \text{or} \quad GA_2(U_y' - \omega_3) + GA_{2r}\left(\omega_1' + \frac{\omega_3}{R} + f\right), \tag{21a}$$

$$\delta\omega_1 = 0 \quad \text{or} \quad GJ\left(\omega_1' + \frac{\omega_3}{R}\right) + GA_r\left(\omega_1' + \frac{\omega_3}{R} + f\right) + GA_{2r}(U_y' - \omega_3) = 0, \tag{21b}$$

$$\delta\omega_3 = 0 \quad \text{or} \quad E\hat{I}_3\left(\omega_3' - \frac{\omega_1}{R}\right) - E\hat{I}_{\phi 3}f' = 0, \tag{21c}$$

$$\delta f = 0 \quad \text{or} \quad E\hat{I}_\phi f' - E\hat{I}_{\phi 3}\left(\omega_3' - \frac{\omega_1}{R}\right) = 0. \tag{21d}$$

On the other hand, Cortinez et al. [22] and Piovan et al. [23] derived the governing equations neglecting the underlined terms in Eqs. (20a)–(20d) for the out-of-plane free vibration of curved

beam. In case of simply supported conditions, (21) is reduced to

$$\delta U_y = 0, \quad \delta\omega_1 = 0,$$

$$M_2 = E\hat{I}_3\left(\omega_3' - \frac{\omega_1}{R}\right) - E\hat{I}_{\phi 3} f' = 0,$$

$$M_\phi = E\hat{I}_\phi f' - E\hat{I}_{\phi 3}\left(\omega_3' - \frac{\omega_1}{R}\right) = 0. \tag{22a–d}$$

Now the lateral displacement, flexural rotation, the torsional rotation, and the warping parameter for out-of-plane vibration of simply supported circular arches can be assumed, respectively, as follows:

$$U_y = A_n \sin\lambda x, \ \omega_3 = B_n \cos\lambda x, \ \omega_1 = C_n \sin\lambda x, \ f = D_n \cos\lambda x, \ n = 1, 2, 3, \ldots, \tag{23a–d}$$

where $\lambda = n\pi/L$. A_n, B_n, C_n, D_n are unknown coefficients. Substituting displacement functions into Eq. (20) and arranging yields

$$\begin{bmatrix} k_{11} & k_{12} & k_{13} & k_{14} \\ & k_{22} & k_{23} & k_{24} \\ & & k_{33} & k_{34} \\ & symn. & & k_{44} \end{bmatrix} \begin{pmatrix} A_n \\ B_n \\ C_n \\ D_n \end{pmatrix} = \begin{pmatrix} 0 \\ 0 \\ 0 \\ 0 \end{pmatrix}, \tag{24}$$

where

$$k_{11} = GA_2\lambda^2 + \rho\omega^2 A,$$
$$k_{12} = \frac{(GA_{2r} - GA_2 R)\lambda}{R},$$
$$k_{13} = GA_{2r}\lambda^2 + \rho\omega^2 \frac{I_2}{R},$$
$$k_{14} = GA_{2r}\lambda,$$
$$k_{22} = E\hat{I}_3\lambda^2 + \frac{(GA_r + GJ - 2GA_{2r}R + GA_2R^2)}{R^2} - \rho\omega^2\tilde{I}_{\phi 3},$$
$$k_{23} = \frac{E\hat{I}_3\lambda}{R} + \frac{(GA_r + GJ - GA_{2r}R)\lambda}{R},$$
$$k_{24} = -E\hat{I}_{\phi 3}\lambda^2 + \frac{(GA_r - GA_{2r}R)}{R} + \rho\omega^2\tilde{I}_{\phi 3},$$
$$k_{33} = \frac{E\hat{I}_3}{R^2} + (GA_r + GJ)\lambda^2 - \rho\omega^2\tilde{I}_0,$$
$$k_{34} = \frac{-E\hat{I}_{\phi 3}\lambda}{R} + GA_r\lambda,$$
$$k_{44} = E\hat{I}_\phi\lambda^2 + GA_r - \rho\omega^2\tilde{I}_\phi. \tag{25a–j}$$

Then the characteristic equation is obtained by taking the determinant of Eq. (24). Here it should be noticed that natural frequencies evaluated from Eq. (24) are exact solutions because not only the displacement functions (23) satisfy both governing equations (20) and boundary conditions (22) but also they minimize the total potential energy.

4. Isoparametric thin-walled curved beam elements

In this section, isoparametric curved beam elements having arbitrary thin-walled cross-sections are presented. The element has seven degrees of freedom per a node. Generally the reduced integration scheme is adopted to avoid the shear-locking phenomena.

Fig. 3 shows the nodal displacement vector of three-noded isoparametric thin-walled curved beam element. In this study, two-, three-, and four-noded isoparametric curved beam element are introduced to interpolate displacement parameters that are defined at the centroid axis. Resultantly, the co-ordinate and all the displacement parameters of the *curved* beam element can be interpolated with respect to the nodal co-ordinates and displacements, respectively, as follows:

$$x_1 = \frac{L}{2}(1+r), \tag{26a}$$

$$U_i = \sum_{\alpha=1}^{n} N_\alpha(r) U_i^\alpha, \quad i = x, y, z, \tag{26b}$$

$$\omega_i = \sum_{\alpha=1}^{n} N_\alpha(r) \omega_i^\alpha, \quad i = 1, 2, 3, \tag{26c}$$

$$f = \sum_{\alpha=1}^{n} N_\alpha(r) f^\alpha, \tag{26d}$$

where n is the total number of node a element, U_i^α, ω_i^α and f^α are the translational and rotational displacements in the x_i direction and warping parameter at node α, respectively, N_α is the isoparametric interpolation function whose the detailed expression is presented in Bathe [38], r is a natural co-ordinate that varies from -1 to $+1$.

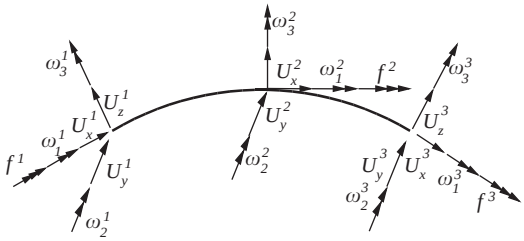

Fig. 3. Nodal displacement vector of three-noded isoparametric curved beam element.

Substituting the shape functions, cross-sectional properties into Eqs. (16) and (17) and integrating along the element length, the total potential energy of thin-walled curved beam element is obtained in matrix form as

$$\Pi = \tfrac{1}{2}\mathbf{U}_e^{\mathrm{T}}(\mathbf{K}_e - \omega^2\mathbf{M}_e)\mathbf{U}_e, \tag{27}$$

where $\mathbf{K}_e$ and $\mathbf{M}_e$ are element elastic stiffness and mass matrices in local co-ordinate, respectively. $\mathbf{U}_e$ is nodal displacement vector which is defined as

$$\mathbf{U}_e = [U^1, U^2, \ldots, U^n], \tag{28a}$$

$$\mathbf{U}^\alpha = [U_x^\alpha, U_y^\alpha, U_z^\alpha, \omega_1^\alpha, \omega_2^\alpha, \omega_3^\alpha, f^\alpha]^{\mathrm{T}}, \quad \alpha = 1, 2, \ldots, n, \tag{28b}$$

where elastic stiffness matrix is evaluated using a reduced Gauss numerical integration scheme.

Now using direct stiffness method, the matrix equilibrium equation for the free vibration analysis of non-symmetric thin-walled curved beam is obtained as

$$\mathbf{K}_E\mathbf{U} = \omega^2\mathbf{M}_E\mathbf{U}, \tag{29}$$

where $\mathbf{K}_E$ and $\mathbf{M}_E$ are global elastic stiffness and mass matrices, respectively.

5. Numerical examples

Closed-form solutions and numerical results analyzed by the curved beam element are presented and compared with other researchers' analytical solutions and results by shell element of ABAQUS [39]. Also, parametric studies for spatial free vibration of curved beams with respect to various subtended angle and boundary conditions are performed in this section.

5.1. Convergence study

To examine the convergence properties of the isoparametric thin-walled curved beams developed by this study, we consider a simply supported curved beam with monosymmetric cross-section for the x_3 axis. The geometric and material data are given in Fig. 4, in which the subtended angle θ_0 is taken to be 90° and the length of beam l is 250 cm.

The convergence study using two-, three- and four-noded isoparametric curved beam elements is performed for in-plane and out-of-plane free vibrational cases and Figs. 5 and 6 show plots of a number of elements versus fundamental in-plane and out-of-plane normalized frequencies, respectively, where ω_{30}^2 denotes the frequency obtained by 30 four-noded isoparametric curved beam elements. It may be noticed that the convergence speeds of both three and four-noded elements are much higher than those of two-noded element for two cases. Furthermore, convergence speeds for out-of-plane frequency are higher than those for in-plane frequency. With five elements, the ratios ω^2/ω_{30}^2 are 1.823, 1.013 and 1.000 for two-, three- and four-noded elements, respectively for in-plane frequencies and 1.299, 1.002 and 1.000 for out-of-plane frequencies. Based on results of this convergence study, in subsequent examples on the free vibrational problems of thin-walled curved beam, a curved beam is modelled by 20 three-noded curved beam elements.

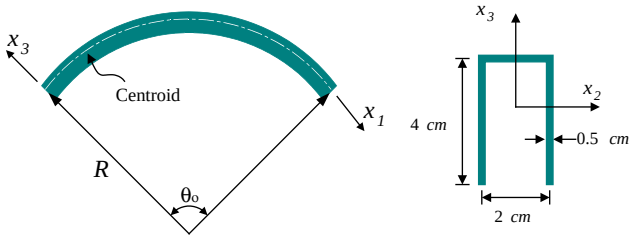

(a) (b)

$A = 5.0\ \text{cm}^2$, $E = 73{,}000\ \text{kg/cm}^2$, $G = 28{,}000\ \text{kg/cm}^2$, $\rho = 0.00785\ \text{kg/cm}^3$, $J = 0.41667\ \text{cm}^4$,
$e_2 = 0\ \text{cm}$, $e_3 = 3.44615\ \text{cm}$, $I_2 = 8.53333\ \text{cm}^4$, $I_3 = 4.33333\ \text{cm}^4$, $I_\phi = 58.02667\ \text{cm}^6$,
$I_{\phi 3} = -14.9333\ \text{cm}^5$, $I_{222} = -2.56\ \text{cm}^5$, $I_{233} = -1.06667\ \text{cm}^5$, $I_{\phi\phi 2} = -59.904\ \text{cm}^7$, $I_{\phi 23} = 10.24\ \text{cm}^6$,
$A^s_2 = 0.46788\ \text{cm}^2$, $A^s_3 = 3.41344\ \text{cm}^2$, $A^s_r = 3.47515\ \text{cm}^4$

(c)

Fig. 4. Circular curved beam with monosymmetric cross-section: (a) simply supported curved beam; (b) monosymmetric cross-section; (c) material and section properties.

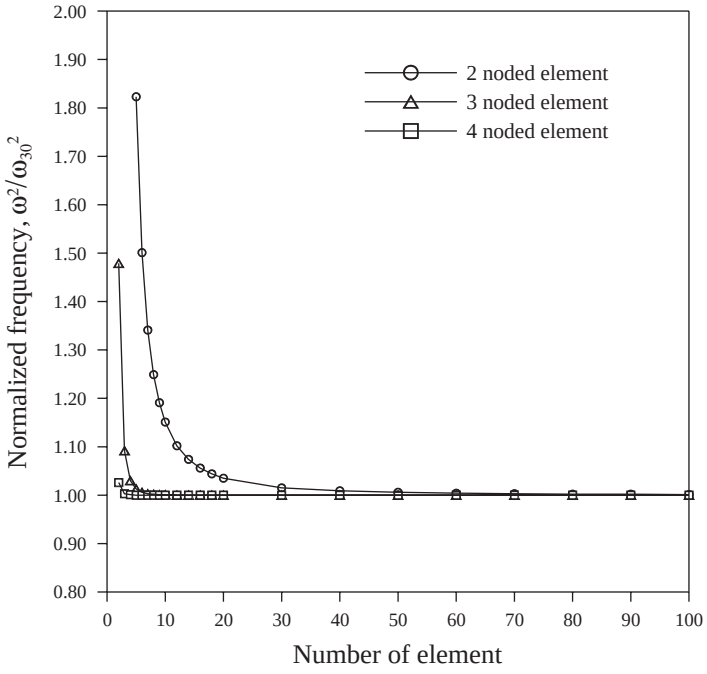

Fig. 5. Convergence of normalized in-plane frequencies.

5.2. *Simply supported curved beam with doubly symmetric cross-sections*

To compare the results by present theory with those by other researchers, in-plane and out-of-plane vibration behaviors of the simply supported curved beam with doubly symmetric

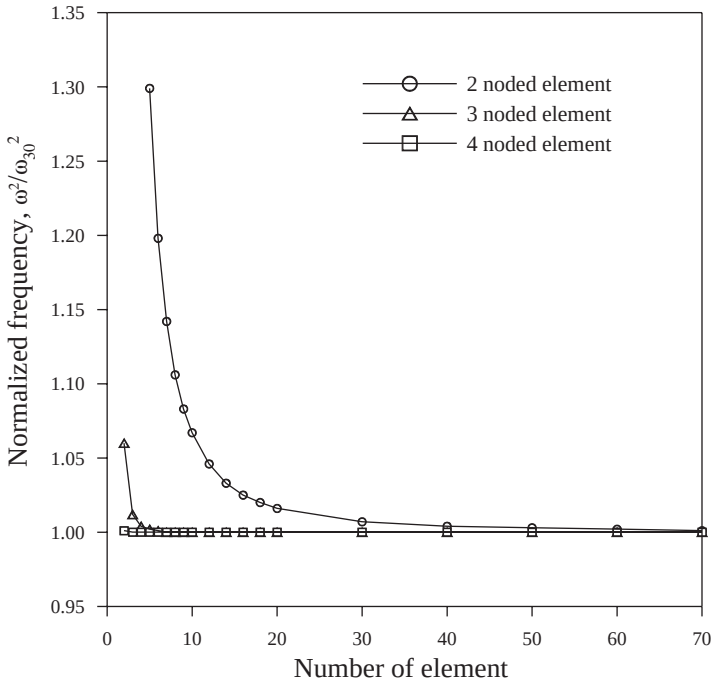

Fig. 6. Convergence of normalized out-of-plane frequencies.

Table 1
In-plane natural frequencies of simply supported doubly symmetric beam (radian/s)^2

Angle (θ_0)	Mode	Present study	Ref. [34]	Ref. [5]
10	1	1550.05	1556.79	1564.99
	2	12416.9	12826.5	12963.4
	3	60005.7	64335.5	65897.8
	4	177374.	199312.	207855.
100	1	0.89954	0.89976	0.89978
	2	5.20058	5.20297	5.20349
	3	19.0033	19.0120	19.0183
	4	46.7508	46.7534	46.7779

cross-sections are examined. First consider in-plane vibration of curved beams with square cross-section whose subtended angle is 10° and 100° with the constant radius. Material and geometric data used for analysis are follows:

$$E = 73,000 \text{ kg/cm}^2, \quad \rho = 0.00785 \text{ kg/cm}^2, \quad b = h = 1 \text{ cm}, \quad R = 100 \text{ cm}.$$

Numerical solutions by this study for the lowest four frequencies are presented in Table 1 with solutions by the previous study [34] neglecting only shear deformation and results by Chidamparam and Leissa [5] neglecting effects of shear deformation, rotary inertia and thickness curvature. Table 1 shows that the maximum difference of the present results with those by the

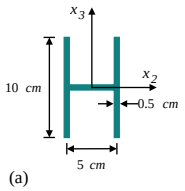

(a)

(b)

$A = 12.5\ \text{cm}^2$, $E = 73{,}000\ \text{kg/cm}^2$, $G = 28{,}000\ \text{kg/cm}^2$, $\rho = 0.00785\ \text{kg/cm}^3$, $J = 1.04167\ \text{cm}^4$,
$e_2 = 0\ \text{cm}$, $e_3 = 0\ \text{cm}$, $I_2 = 83.3333\ \text{cm}^4$, $I_3 = 67.7083\ \text{cm}^4$, $I_\phi = 520.833\ \text{cm}^6$,
$I_{\phi 23} = 520.833\ \text{cm}^6$, $l = 200\ \text{cm}$, $A^s_2 = 1.94521\ \text{cm}^2$, $A^s_3 = 8.33333\ \text{cm}^2$, $A^s_r = 52.0834\ \text{cm}^4$

Fig. 7. Profile of H shaped cross-section and material and section properties: (a) H shaped cross section; (b) material and section properties.

Table 2
Out-of-plane natural frequencies for the simply supported doubly symmetric beam (radian/s)^2 ($L = 200$ cm)

Angle (θ_0)	Mode (n)	Present study		Ref. [23]
		Analytic solution	F.E. solution	
10	1	1.9634	1.9634	1.9700
	2	37.974	37.976	38.116
	3	181.47	181.51	182.19
	4	519.25	519.65	521.12
90	1	0.0515	0.0515	0.0723
	2	6.5659	6.5665	7.5920
	3	71.853	71.879	78.449
	4	302.10	302.40	322.77
180	1	0.0000	0.0000	0.0000
	2	1.3263	1.3265	2.5528
	3	26.795	26.807	37.449
	4	161.64	161.84	199.51

previous study [34] and with Chidamparam and Leissa's results are 12.4% and 17.2%, respectively, at the fourth natural frequency for the angle is 10°.

Next, the out-of-plane natural frequencies of simply supported curved beam with H shaped cross-section having various subtended angles but the constant length of beam is evaluated. The geometric and material data for analysis are given in Fig. 7. Closed-form solutions based on the governing equation (20) and numerical solutions are presented in Table 2 with the result following the governing equation given by Piovan et al. [23] which neglect the underlined terms in (20). From Table 2, it is found that there are some differences for a small subtended angle between this study and the result by Piovan et al. Particularly, the difference becomes large with increase of the subtended angle up to the maximum difference 92.5% at the frequency corresponding to two half sine waves for the subtended angle $\theta_0 = 180°$.

5.3. *Thin-walled curved beam with monosymmetric section x_3-axis*

In this example, in-plane and out-of-plane vibrational behaviors of curved beams are investigated through the various parametric studies. The same geometric and material data of curved beam as the one used in the example 5.1 are adopted (see Fig. 4).

Table 3 shows the first five in-plane natural frequencies with respect to the various subtended angles for simply supported curved beams whose length is 50 and 200 cm, respectively. For comparison, the results by 20 cubic Hermitian beam elements without shear deformation effect are together presented. And also, in Table 4 is listed the first five out-of-plane natural frequencies by the closed-form solution with shear deformation and by the numerical solution with and without shear deformation. It can be noticed that not only relative differences of frequencies due shear deformation effects are large in higher vibrational modes but also the closed-form solutions are in a good agreement with the results by curved beam element in the whole range of subtended angles.

The fundamental in-plane symmetric and antisymmetric frequencies for the simply supported (S–S) and clamped (C–C) curved beams of length $l = 100$ cm versus various subtended angles have been plotted in Fig. 8. As shown in Fig. 8, the antisymmetric frequencies decrease slowly as the subtended angle increases whereas the symmetric frequencies experience a sharp increase. Also

Table 3
In-plane natural frequencies for the simply supported monosymmetric beam (radian/s)^2

Length	Angle (θ_0)	Mode	With shear deformation	Without shear deformation
50	30	1	1041.96	1048.64
		2	3398.32	3731.69
		3	15613.7	18850.2
		4	36737.3	37264.3
		5	43238.4	57386.0
	90	1	2610.44	2869.24
		2	6686.94	6893.78
		3	15931.4	18767.3
		4	35904.5	40589.4
		5	49058.0	58828.1
	180	1	1147.45	1265.21
		2	8981.06	10787.5
		3	31214.9	34479.5
		4	33400.2	40603.0
		5	68574.1	73140.7
200	30	1	14.8261	14.9206
		2	44.3843	44.5777
		3	89.7269	90.6257
		4	237.870	243.762
		5	576.534	598.278
	90	1	11.3731	11.4458
		2	61.4545	62.3146
		3	222.826	228.350
		4	445.721	453.289
		5	650.445	664.558
	180	1	4.94910	4.98098
		2	45.6069	46.2587
		3	183.525	188.096
		4	476.864	494.805
		5	1038.69	1093.71

Table 4
Out-of-plane natural frequencies for the simply supported monosymmetric beam (radian/s)^2

Length	Angle (θ_0)	Mode (n)	Analytic solution	F.E. solution	
				With shear deformation	Without shear deformation
50	30	1	102.591	102.591	111.133
		2	516.113	516.130	558.077
		3	553.314	553.315	576.594
		4	1475.40	1475.67	1789.61
		5	3298.78	3300.75	4507.84
	90	1	22.6827	22.6829	23.3032
		2	861.117	861.135	1014.20
		3	1511.18	1511.18	1605.78
		4	1875.86	1876.15	2328.27
		5	3794.64	3796.71	4957.10
	180	1	0.00000	0.00000	0.00000
		2	763.880	763.956	946.746
		3	2617.22	2617.51	3353.05
		4	3162.78	3162.79	3490.99
		5	4586.99	4589.14	6456.94
200	30	1	0.34351	0.34352	0.34495
		2	7.43988	7.44025	7.61160
		3	28.8676	28.8735	30.0129
		4	38.6432	38.6432	38.7100
		5	65.5991	65.6371	68.9167
	90	1	0.04343	0.04343	0.04346
		2	4.39389	4.39424	4.45395
		3	35.7129	35.7228	37.5227
		4	92.0290	92.0804	98.7250
		5	158.050	158.237	170.521
	180	1	0.00000	0.00000	0.00000
		2	0.87041	0.87050	0.87389
		3	17.0762	17.0841	17.5055
		4	98.2060	98.3089	106.156
		5	222.706	222.994	248.870

this figure exhibits the phenomenon of mode crossover, which occurs at the crossing of symmetric and antisymmetric natural frequency curves. The crossover occurs at the subtended angle around $\theta_0 = 31^\circ,\ 50^\circ$ for simply supported and clamped conditions, respectively. Furthermore, after the crossover point is passed, it is observed that frequencies corresponding to the symmetric mode increase rapidly and then change very slowly as the subtended angle increases further. In this range, it turns out that the symmetric mode having one half-wave is transformed into the symmetric mode with three half-waves (see Fig. 9). This is called *mode transition* phenomenon for the symmetric in-plane vibrational mode of simply supported curved beams. A similar situation occurs for the clamped ends.

Now, effects of shear deformation on the in-plane natural frequencies are examined. Fig. 10 shows relative differences of the fundamental in-plane frequencies due to shear deformation with

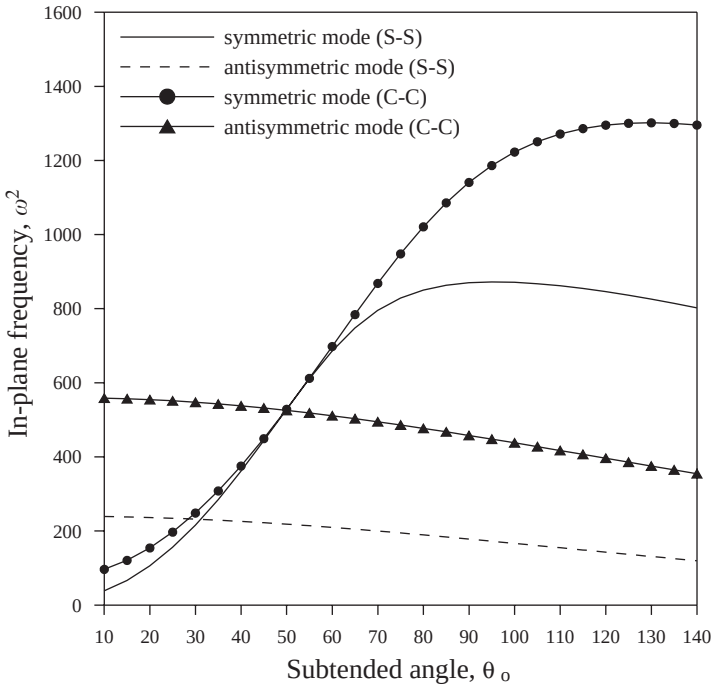

Fig. 8. In-plane frequency with subtended angle ($l = 100$ cm).

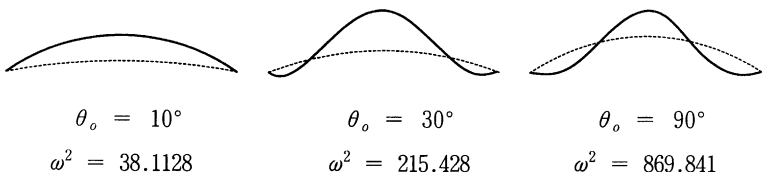

Fig. 9. Mode transition of fundamental symmetric vibrational modes for the simply supported curved beam.

the increase of subtended angles for simply supported and clamped ends, respectively, in which ω^{*2} denotes the natural frequency neglecting shear deformation. It is interesting to note that effect of shear deformation jumps upward at the point of crossover for simply supported and clamped ends. In the low range of subtended angle, effect of shear deformation is small because the fundamental vibrational mode is symmetric mode with one half-wave as can be seen Fig. 9. However after the crossover point, the fundamental mode changes into the antisymmetric mode with two half-waves, in which shear deformation effect is large. Also it can be found that the shear deformation effect of curved beam with clamped ends is not always larger than that of simply supported curved beam in the whole range of subtended angles due to the phenomenon of crossover mentioned above. In addition, shear deformation effect of the antisymmetric mode is almost constant with increase of subtended angle for both boundary conditions.

Next Figs. 11 and 12 show the out-of-plane symmetric and antisymmetric frequencies of curved beam with simply supported ends versus various subtended angle and relative differences of the fundamental out-of-plane frequency due to shear deformation, respectively. From Fig. 11, it can

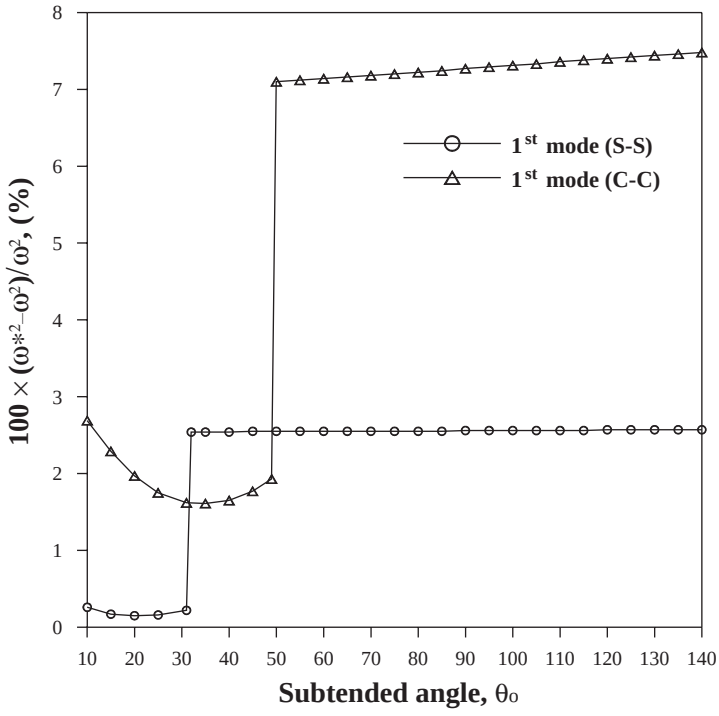

Fig. 10. Effect of shear deformation of fundamental in-plane frequency with subtended angle.

be found that the crossover of symmetric and antisymmetric out-of-plane frequency curves occurs at the subtended angle of around $\theta_0 = 320^\circ$. Also the effect of shear deformation jumps upward at the crossover point (Fig. 12). This phenomenon is due to the fact that the fundamental vibrational mode is interchanged from the symmetric mode with one half-wave into the antisymmetric mode with two half-waves at the crossover point.

5.4. Clamped semicircular beams with Z-sections

This example considers the clamped semicircular beam with Z-section of equal flanges as shown in Fig. 13. Table 5 shows the lowest five spatially coupled natural frequencies by present study. For comparison, the numerical solutions [34] neglecting shear deformation and the results by the Gendy and Saleeb [33] and those by the shell element model of Noor et al. [40] are together presented. From Table 5, it is observed that the results by the present study are slightly better than those by Gendy and Saleeb's model when comparing with those using the shell element. Also the maximum difference of results by this study and those by Gendy and Saleeb' model is 6.4% at third vibrational mode.

5.5. Cantilever and clamped curved beams with non-symmetric cross-sections

In this example, the spatially coupled free vibration analysis of non-symmetric curved beams with clamped–free and clamped–clamped ends is performed for various subtended angles. Fig. 14

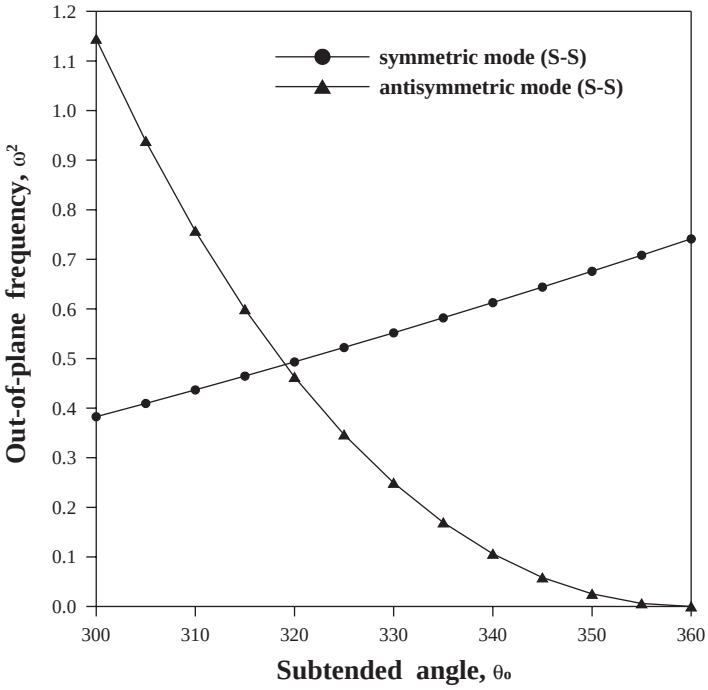

Fig. 11. Out-of-plane frequency with subtended angle ($l = 100$ cm).

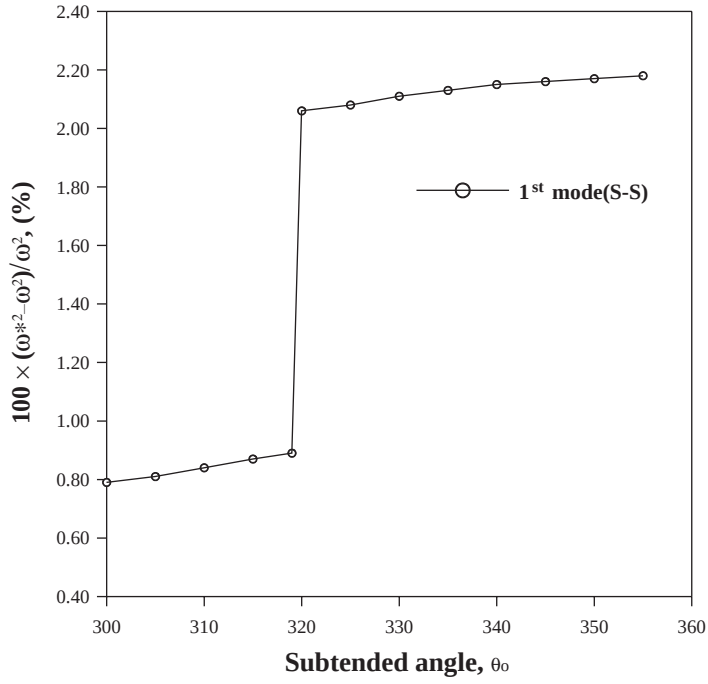

Fig. 12. Effect of shear deformation of fundamental out-of-plane frequency with subtended angle.

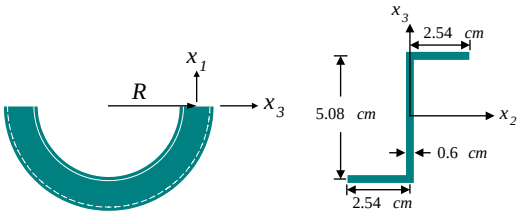

(a) (b)

$A = 6.096\ \text{cm}^2$, $E = 730{,}887\ \text{kg/cm}^2$, $G = 281{,}110\ \text{kg/cm}^2$, $\rho = 0.002768\ \text{kg/cm}^3$, $J = 0.73152\ \text{cm}^4$,
$e_2 = 0\ \text{cm}$, $e_3 = 0\ \text{cm}$, $I_2 = 26.2193\ \text{cm}^4$, $I_3 = 6.55483\ \text{cm}^4$, $I_\phi = 26.4307\ \text{cm}^6$, $I_{\phi 2} = -21.1446\ \text{cm}^5$,
$I_{\phi 3} = -21.1446\ \text{cm}^5$, $I_{\phi 23} = -26.4307\ \text{cm}^5$, $R = 100.0\ \text{cm}$
$A^s_2 = 2.32404\ \text{cm}^2$, $A^s_3 = 2.89801\ \text{cm}^2$, $A^s_r = 12.0494\ \text{cm}^4$

(c)

Fig. 13. Clamped semicircular curved beam with Z cross-section: (a) clamped curved beam; (b) non-symmetric Z cross-section; (c) material and section properties.

Table 5
Natural frequencies of clamped semicircular beam $(\text{radian/s})^2$

Mode	Present study	Ref. [34]	Ref. [33]	Ref. [40]
1	4.8198	4.8963	4.8993	4.5199
2	23.119	23.252	23.852	22.777
3	107.22	107.90	114.06	105.60
4	162.93	166.50	168.55	156.79
5	333.93	336.97	335.82	329.87

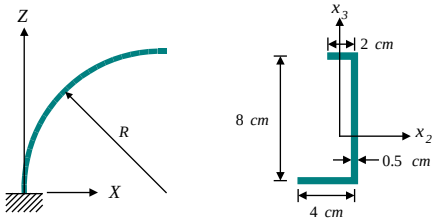

(a) (b)

$A = 7.0\ \text{cm}^2$, $E = 30{,}000\ \text{kg/cm}^2$, $G = 11{,}500\ \text{kg/cm}^2$, $J = 0.5833\ \text{cm}^4$, $\rho = 0.00785\ \text{kg/cm}^3$,
$I_2 = 67.0476\ \text{cm}^4$, $I_3 = 8.4286\ \text{cm}^4$, $I_{23} = 9.1429\ \text{cm}^4$, $I_{222} = 52.2449\ \text{cm}^5$, $I_{223} = -20.0272\ \text{cm}^5$,
$I_{233} = -17.4150\ \text{cm}^5$, $I_{333} = -13.3878\ \text{cm}^5$, $I_\phi = 272.5442\ \text{cm}^6$, $I_{\phi 2} = 115.8095\ \text{cm}^5$, $I_{\phi 3} = 30.4762\ \text{cm}^5$,
$I_{\phi 22} = 59.2109\ \text{cm}^6$, $I_{\phi 23} = -107.1020\ \text{cm}^6$, $I_{\phi 33} = -63.1293\ \text{cm}^6$, $I_{\phi\phi 2} = -67.1720\ \text{cm}^7$, $I_{\phi\phi 3} = -388.7269\ \text{cm}^7$,
$A^s_2 = 1.6935\ \text{cm}^2$, $A^s_3 = 3.4815\ \text{cm}^2$, $A^s_r = 26.7079\ \text{cm}^4$

(c)

Fig. 14. Cantilever curved beam with non-symmetric cross-section: (a) geometry of curved beam; (b) cross-section; (c) material and section properties.

Table 6
Natural frequencies of non-symmetric cantilever curved beam (radian/s)^2

Angle (θ_0)	Method	Vibration mode									
		1	2	3	4	5	6	7	8	9	10
10	Present study	0.0289	0.2672	0.5938	1.5157	5.0785	7.5997	16.973	20.192	26.497	50.875
	Ref. [34]	0.0290	0.2686	0.5963	1.5252	5.1373	7.7438	17.386	20.623	27.159	52.344
30	Present study	0.0211	0.2798	0.3737	2.2526	4.9884	7.2984	19.109	20.051	27.454	47.676
	Ref. [34]	0.0212	0.2815	0.3747	2.2666	5.0554	7.4328	19.493	20.511	28.177	49.067
60	Present study	0.0107	0.2470	0.3067	2.3617	5.6800	7.0548	17.886	27.702	30.422	43.573
	Ref. [34]	0.0107	0.2480	0.3084	2.3788	5.8332	7.1242	18.221	28.219	31.322	44.828
90	Present study	0.0062	0.2051	0.2883	2.0111	5.0525	7.2818	17.197	31.627	37.201	46.719
	Ref. [34]	0.0062	0.2061	0.2901	2.0272	5.2139	7.3646	17.473	32.844	37.949	47.721
	ABAQUS [39]	0.0060	0.2043	0.2779	1.9714	5.0293	7.1815	17.079	32.233	36.624	43.574
120	Present study	0.0042	0.1598	0.2929	1.6744	4.2126	6.9482	16.484	32.775	35.555	66.874
	Ref. [34]	0.0043	0.1608	0.2945	1.6893	4.3515	7.0502	16.728	34.383	36.373	67.954
150	Present study	0.0034	0.1213	0.3127	1.3800	3.5354	6.3441	15.567	31.995	33.572	66.454
	Ref. [34]	0.0034	0.1222	0.3141	1.3938	3.6529	6.4512	15.798	33.813	34.377	68.559
180	Present study	0.0030	0.0922	0.3447	1.1265	3.0410	5.6769	14.500	29.706	31.903	62.142
	Ref. [34]	0.0030	0.0929	0.3462	1.1389	3.1403	5.7825	14.724	31.503	32.765	64.026

shows a non-symmetric curved cantilever beam and its material and sectional properties. In Tables 6 and 7, the lowest 10 frequencies of curved cantilever and clamped–clamped curved beams of length $l = 200$ cm are presented with respect to the various subtended angles. The solutions by present study, the solutions [34] neglecting shear deformation and the results by 300 shell elements of ABAQUS which is the commercial F.E. analysis program are presented for comparison. From tables, it is shown that the results by present method are in a good agreement with those by ABAQUS's shell elements. As shown in Table 6, for the curved cantilever beam, the maximum difference of frequencies due to shear deformation is 6.0% at the eighth mode for the subtended angle $\theta_0 = 180^\circ$. Also it is observed that the shear deformation effects in the clamped–clamped curved beam are relatively larger than those in the cantilever beam and the maximum difference is 12.9% at the tenth mode for the subtended angle $\theta_0 = 10^\circ$.

6. Conclusions

For spatial free vibration analysis of shear deformable curved beams having arbitrary thin-walled cross-sections, an improved theory is formulated. The closed-form solution for out-of-plane vibrational deformations of monosymmetric circular beams is newly derived and the isoparametric curved beam elements are developed. The closed-form and the F.E. solutions by the

Table 7
Natural frequencies of non-symmetric clamped curved beam (radian/s)^2

Angle (θ_0)	Method	Vibration mode									
		1	2	3	4	5	6	7	8	9	10
10	Present study	0.9388	4.3755	6.2020	16.887	18.361	20.637	47.850	57.241	95.128	105.91
	Ref. [34]	0.9488	4.4120	6.3262	17.732	18.778	21.295	49.634	59.534	99.775	119.58
30	Present study	0.8264	5.2791	10.645	17.672	21.490	30.441	43.626	65.695	88.794	110.16
	Ref. [34]	0.8338	5.3737	10.799	18.125	22.087	31.469	45.206	68.388	93.079	123.91
60	Present study	0.7681	4.4271	15.044	23.538	26.510	38.338	58.008	80.708	101.98	117.80
	Ref. [34]	0.7753	4.4992	15.392	24.041	27.515	39.667	60.538	84.626	104.35	131.16
90	Present study	0.7134	3.9278	13.272	30.219	34.103	41.075	67.752	76.159	128.49	137.44
	Ref. [34]	0.7223	3.9916	13.570	31.829	35.223	41.852	71.047	80.568	138.20	148.88
	ABAQUS [39]	0.7020	3.9088	13.388	30.838	34.855	37.792	69.831	78.659	115.15	140.53
120	Present study	0.6344	3.5618	11.986	30.249	31.713	63.380	66.200	79.918	124.23	151.78
	Ref. [34]	0.6446	3.6238	12.257	31.523	33.616	64.519	68.869	86.169	130.81	165.18
150	Present study	0.5420	3.2285	10.998	27.214	30.484	60.262	83.318	94.335	115.54	180.24
	Ref. [34]	0.5522	3.2906	11.259	28.378	32.733	62.680	90.153	96.772	121.55	193.33
180	Present study	0.4495	2.8955	10.162	24.061	28.316	55.990	84.329	107.63	129.94	188.48
	Ref. [34]	0.4589	2.9571	10.422	25.347	30.400	58.225	93.334	113.14	131.99	200.85

present study are compared with other researchers' results and numerical results using ABAQUS's shell elements and the parametric study is performed. Consequently, conclusions drawn from this study are as follows:

1. *Mode transition* phenomena from the symmetric mode having one half-wave to the symmetric mode with three half-waves are observed in case of in-plane free vibration of simply supported and clamped curved beams. In this case, shear deformation effects increase sharply around the mode transition point due to the increase of the half-wave number.
2. Crossover phenomena are detected for out-of-plane vibrational mode as well as in-plane mode of monosymmetric curved beams.
3. For spatially coupled free vibration problem of non-symmetric thin-walled cantilever and clamped curved beams, it is shown that the numerical solutions by the isoparametric curved beam element considering shear effects are in a good agreement with the results by shell elements of ABAQUS.

Acknowledgements

The authors are grateful for the support provided by a grant (R01-2002-000-00265-0) from the Korea Science and Engineering Foundation (KOSEF) and the Brain Korea 21 Project.

Appendix A

Equations of motion and boundary conditions for shear deformable curved beams are given as follows:

$$
\begin{aligned}
&-EA\left(U_x'' + \frac{1}{R}U_z'\right) + \frac{1}{R}E\hat{I}_2\left(\omega_2'' - \frac{1}{R}U_x'' - \frac{1}{R^2}U_z'\right) + \frac{1}{R}E\hat{I}_{\phi 2}f'' \\
&\quad - \frac{1}{R}E\hat{I}_{23}\left(\omega_3'' - \frac{1}{R}\omega_1'\right) - \frac{1}{R}GA_3\left(U_z' + \omega_2 - \frac{1}{R}U_x\right) - \frac{1}{R}GA_{23}(U_y' - \omega_3) \\
&\quad - \frac{1}{R}GA_{3r}\left(\omega_1' + f + \frac{1}{R}\omega_3\right) \\
&\quad = \rho\omega^2\left(AU_x + \frac{1}{R}I_2\omega_2 - \frac{1}{R}I_{23}\omega_3 + \frac{1}{R}I_{\phi 2}f\right),
\end{aligned} \tag{A.1}
$$

$$
\begin{aligned}
&-GA_2(U_y'' - \omega_3') - GA_{23}\left(U_z'' + \omega_2' - \frac{1}{R}U_x'\right) - GA_{2r}\left(\omega_1'' + f' + \frac{1}{R}\omega_3'\right) \\
&\quad = \rho\omega^2\left(AU_y - \frac{1}{R}I_2\omega_1\right),
\end{aligned} \tag{A.2}
$$

$$
\begin{aligned}
&\frac{1}{R}EA\left(U_x' + \frac{1}{R}U_z\right) - \frac{1}{R^2}E\hat{I}_2\left(\omega_2' - \frac{1}{R}U_x' - \frac{1}{R^2}U_z\right) - \frac{1}{R^2}E\hat{I}_{\phi 2}f' \\
&\quad + \frac{1}{R^2}E\hat{I}_{23}\left(\omega_3' - \frac{1}{R}\omega_1\right) - GA_3\left(U_z'' + \omega_2' - \frac{1}{R}U_x'\right) - GA_{23}(U_y'' - \omega_3') \\
&\quad - GA_{3r}\left(\omega_1'' + f' + \frac{1}{R}\omega_3'\right) = \rho\omega^2\left(AU_z + \frac{1}{R}I_{23}\omega_1\right),
\end{aligned} \tag{A.3}
$$

$$
\begin{aligned}
&-\frac{1}{R}E\hat{I}_3\left(\omega_3' - \frac{1}{R}\omega_1\right) + \frac{1}{R}E\hat{I}_{\phi 3}f' + \frac{1}{R}E\hat{I}_{23}\left(\omega_2' - \frac{1}{R}U_x' - \frac{1}{R^2}U_z\right) \\
&\quad - GJ\left(\omega_1'' + \frac{1}{R}\omega_3'\right) - GA_r\left(\omega_1'' + f' + \frac{1}{R}\omega_3'\right) - GA_{2r}(U_y'' - \omega_3') \\
&\quad - GA_{3r}\left(U_z'' + \omega_2' - \frac{1}{R}U_x'\right) = \rho\omega^2\left(\tilde{I}_0\omega_1 - \frac{1}{R}I_2U_y + \frac{1}{R}I_{23}U_z\right),
\end{aligned} \tag{A.4}
$$

$$
\begin{aligned}
&-E\hat{I}_2\left(\omega_2'' - \frac{1}{R}U_x'' - \frac{1}{R^2}U_z'\right) - E\hat{I}_{\phi 2}f'' + E\hat{I}_{23}\left(\omega_3'' - \frac{1}{R}\omega_1'\right) \\
&\quad + GA_3\left(U_z' + \omega_2 - \frac{1}{R}U_x\right) + GA_{23}(U_y' - \omega_3) + GA_{3r}\left(\omega_1' + f + \frac{1}{R}\omega_3\right) \\
&\quad = \rho\omega^2\left(\tilde{I}_2\omega_2 + \frac{1}{R}I_2U_x - \tilde{I}_{23}\omega_3 + \tilde{I}_{\phi 2}f\right),
\end{aligned} \tag{A.5}
$$

$$
\begin{aligned}
&- E\hat{I}_3\left(\omega_3'' - \frac{1}{R}\omega_1'\right) + E\hat{I}_{\phi 3}f'' + E\hat{I}_{23}\left(\omega_2'' - \frac{1}{R}U_x'' - \frac{1}{R^2}U_z'\right)\\
&+ \frac{1}{R}GJ\left(\omega_1' + \frac{1}{R}\omega_3\right) - GA_2(U_y' - \omega_3) - GA_{23}\left(U_z' + \omega_2 - \frac{1}{R}U_x\right)\\
&+ \frac{1}{R}GA_r\left(\omega_1' + f + \frac{1}{R}\omega_3\right) + \frac{GA_{3r}}{R}\left(U_z' + \omega_2 - \frac{1}{R}U_x\right)\\
&- GA_{2r}\left(\omega_1' + f - \frac{1}{R}U_y' + \frac{2}{R}\omega_3\right)\\
&= \rho\omega^2\left(\tilde{I}_3\omega_3 - \frac{1}{R}I_{23}U_x - \tilde{I}_{23}\omega_2 - \tilde{I}_{\phi 3}f\right), \qquad \text{(A.6)}
\end{aligned}
$$

$$
\begin{aligned}
&- E\hat{I}_\phi f'' - E\hat{I}_{\phi 2}\left(\omega_2'' - \frac{1}{R}U_x'' - \frac{1}{R^2}U_z'\right) + E\hat{I}_{\phi 3}\left(\omega_3'' - \frac{1}{R}\omega_1'\right)\\
&+ GA_r\left(\omega_1' + f + \frac{1}{R}\omega_3\right) + GA_{2r}(U_y' - \omega_3) + GA_{3r}\left(U_z' + \omega_2 - \frac{1}{R}U_x\right)\\
&= \rho\omega^2\left(\tilde{I}_\phi f + \tilde{I}_{\phi 2}\omega_2 - \tilde{I}_{\phi 3}\omega_3 + \frac{1}{R}I_{\phi 2}U_x\right), \qquad \text{(A.7)}
\end{aligned}
$$

and

$$\delta U_x(o) = \delta U_x^p \text{ or } F_1(o) = -F_1^p, \quad \delta U_x(l) = \delta U_x^q \text{ or } F_1(l) = F_1^q, \qquad \text{(A.8, 9)}$$

$$\delta U_y(o) = \delta U_y^p \text{ or } F_2(o) = -F_2^p, \quad \delta U_y(l) = \delta U_y^q \text{ or } F_2(l) = F_2^q, \qquad \text{(A.10, 11)}$$

$$\delta U_z(o) = \delta U_z^p \text{ or } F_3(o) = -F_3^p, \quad \delta U_z(l) = \delta U_z^q \text{ or } F_3(l) = F_3^q, \qquad \text{(A.12, 13)}$$

$$\delta\omega_1(o) = \delta\omega_1^p \text{ or } M_1(o) = -M_1^p, \quad \delta\omega_1(l) = \delta\omega_1^q \text{ or } M_1(l) = M_1^q, \qquad \text{(A.14, 15)}$$

$$\delta\omega_2(o) = \delta\omega_2^p \text{ or } M_2(o) = -M_2^p, \quad \delta\omega_2(l) = \delta\omega_2^q \text{ or } M_2(l) = M_2^q, \qquad \text{(A.16, 17)}$$

$$\delta\omega_3(o) = \delta\omega_3^p \text{ or } M_3(o) = -M_3^p, \quad \delta\omega_3(l) = \delta\omega_3^q \text{ or } M_3(l) = M_3^q, \qquad \text{(A.18, 19)}$$

$$\delta f(o) = \delta f^p \text{ or } M_\phi(o) = -M_\phi^p, \quad \delta f(l) = \delta f^q \text{ or } M_\phi(l) = M_\phi^q. \qquad \text{(A.20, 21)}$$

Appendix B

For shear rigid curved beam, the elastic strain energy and the kinetic energy are given as follows:

$$
\begin{aligned}
\Pi_E = \frac{1}{2}\int_0^L \Bigg[& EA\left(U_x' + \frac{U_z}{R}\right)^2 + E\hat{I}_2\left(U_z'' + \frac{U_z}{R^2}\right)^2 + E\hat{I}_3\left(U_y'' - \frac{\theta}{R}\right)^2\\
&+ E\hat{I}_\phi\left(\theta'' + \frac{U_y''}{R}\right)^2 + GJ\left(\theta' + \frac{U_y'}{R}\right)^2 + 2E\hat{I}_{\phi 2}\left(U_z'' + \frac{U_z}{R^2}\right)\left(\theta'' + \frac{U_y''}{R}\right)
\end{aligned}
$$

$$+2E\hat{I}_{\phi 3}\left(U_y''-\frac{\theta}{R}\right)\left(\theta''+\frac{U_y''}{R}\right)$$
$$+2E\hat{I}_{23}\left(U_y''-\frac{\theta}{R}\right)\left(U_z''+\frac{U_z}{R^2}\right)\Bigg]\mathrm{d}x_1, \tag{B.1}$$

$$\Pi_M=\frac{1}{2}\rho\omega^2\int_0^L\Bigg[A(U_x^2+U_y^2+U_z^2)+\tilde{I}_0\theta^2+\tilde{I}_2\left(U_z'-\frac{U_x}{R}\right)^2-2\frac{I_2}{R}U_y\theta$$
$$-2\frac{I_2}{R}U_x\left(U_z'-\frac{U_x}{R}\right)+\tilde{I}_3U_y'^2+\tilde{I}_\phi\left(\theta'+\frac{U_y'}{R}\right)^2+2\tilde{I}_{\phi 3}U_y'\left(\theta'+\frac{U_y'}{R}\right)$$
$$+2\tilde{I}_{\phi 2}\left(U_z'-\frac{U_x}{R}\right)\left(\theta'+\frac{U_y'}{R}\right)-2\frac{I_{\phi 2}}{R}U_x\left(\theta'+\frac{U_y'}{R}\right)$$
$$+2\frac{I_{223}}{R}U_y'\left(U_z'-\frac{U_x}{R}\right)+2I_{23}\left(U_y'U_z'-\frac{2}{R}U_xU_y'+\frac{1}{R}U_z\theta\right)\Bigg]\mathrm{d}x_1. \tag{B.2}$$

References

[1] V.Z. Vlasov, *Thin-walled Elastic Beams*, National Science Foundation, Washington, DC, 1961.
[2] S.P. Timoshenko, J.M. Gere, *Theory of Elastic Stability*, McGraw-Hill, New York, 1961.
[3] T. Tarnopolskaya, F.R. De Hoog, N.H. Fletcher, Low-frequency mode transition in the free in-plane vibration of curved beams, *Journal of Sound and Vibration* 228 (1999) 69–90.
[4] T. Tarnopolskaya, F.R. De Hoog, N.H. Fletcher, S. Thwaites, Asymptotic analysis of the free in-plane vibrations of beam with arbitrarily varying curvature and cross-section, *Journal of Sound and Vibration* 196 (1996) 659–680.
[5] P. Chidamparam, A.W. Leissa, Influence of centerline extensibility on the in-plane free vibrations of loaded circular arches, *Journal of Sound and Vibration* 183 (1995) 779–795.
[6] J.P. Charpie, C.B. Burroughs, An analytic model for the free in-plane vibration of beams of variable curvature and depth, *Journal of the Acoustical Society of America* 94 (1993) 866–879.
[7] J.F.M. Scott, J. Woodhouse, Vibration of an elastic strip with varing curvature, *Philosophical Transactions of the Royal Society of London, Physical Sciences and Engineering* 339 (1992) 587–625.
[8] M. Petyt, C.C. Fleischer, Free vibration of a curved beam, *Journal of Sound and Vibration* 18 (1971) 17–30.
[9] A. Krishnan, Y.J. Suresh, A simple cubic linear element for static and free vibration analysis of curved beams, *Computers & Structures* 68 (1998) 473–489.
[10] C.S. Huang, Y.P. Tseng, A.W. Leissa, K.Y. Nieh, An exact solution for in-plane vibrations of an arch having variable curvature and cross section, *International Journal of Mechanical Sciences* 40 (1998) 1159–1173.
[11] Y.P. Tseng, C.S. Huang, C.J. Lin, Dynamic stiffness analysis for in-plane vibrations of arches with variable curvature, *Journal of Sound and Vibration* 207 (1997) 15–31.
[12] K. Suzuki, S. Takahashi, In-plane vibration of curved bars with varying cross-section, *Bulletin of the Japan Society of Mechanical Engineers* 25 (1982) 1100–1107.
[13] T. Irie, G. Yamada, I. Takahashi, In-plane vibration of a free-clamped slender arc of varying cross-section, *Bulletin of the Japan Society of Mechanical Engineers* 23 (1980) 567–573.
[14] P. Raveendranath, G. Singh, B. Pradhan, Free vibration of arches using a curved beam element based on a coupled polynomial displacement field, *Computers & Structures* 78 (2000) 583–590.
[15] S.J. Oh, B.K. Lee, I.W. Lee, Natural frequencies of non-circular arches with rotatory inertia and shear deformation, *Journal of Sound and Vibration* 219 (1999) 23–33.

[16] A.K. Gupta, W.P. Howson, Exact natural frequencies of plane structures composed of slender elastic curved members, *Journal of Sound and Vibration* 175 (1994) 145–157.
[17] B.K. Lee, J.F. Wilson, Free vibrations of arches with variable curvature, *Journal of Sound and Vibration* 136 (1989) 75–89.
[18] M.S. Issa, T.M. Wang, B.T. Hsiao, Extensional vibrations of continuous circular curved beams with rotary inertia and shear deformation, I: free vibration, *Journal of Sound and Vibration* 114 (1987) 297–308.
[19] T.M. Wang, M.P. Guilbert, Effects of rotary inertia and shear on natural frequencies of continuous circular curved beams, *International Journal of Solids and Structures* 17 (1981) 281–289.
[20] T.M. Wang, Lowest natural frequency of clamped parabolic arcs, *Journal of Structural Division* 98 (1972) 407–411.
[21] A.S. Veletsos, W.J. Austin, C.A. Lopes, Shyr-jen Wung, Free in-plane vibration of circular arches, *Journal of Engineering Mechanics Division* 98 (1972) 311–329.
[22] V.H. Cortinez, M.T. Piovan, R.E. Rossi, Out of plane vibrations of thin walled curved beams considering shear flexibility, *Structural Engineering and Mechanics* 8 (1999) 257–272.
[23] M.T. Piovan, V.H. Cortinez, R.E. Rossi, Out-of-plane vibrations of shear deformable continuous horizontally curved thin-walled beams, *Journal of Sound and Vibration* 237 (2000) 101–118.
[24] W.P. Howson, A.K. Jemah, Exact out-of-plane natural frequencies of curved Timoshenko beams, *Journal of Engineering Mechanics* 125 (1999) 19–25.
[25] W.P. Howson, A.K. Jemah, J.Q. Zhou, Exact natural frequencies for out-of-plane motion of plane structures composed of curved beam members, *Computers & Structures* 55 (1995) 989–995.
[26] J.M. Snyder, J.F. Wilson, Free vibrations of continuous horizontally curved beams, *Journal of Sound and Vibration* 157 (1992) 345–355.
[27] T.M. Wang, W.F. Brannen, Natural frequencies for out-of-plane vibrations of curved beams on elastic foundations, *Journal of Sound and Vibration* 84 (1982) 241–246.
[28] T.M. Wang, R.H. Nettleton, B. Keita, Natural frequencies for out-of-plane vibrations of continuous curved beams, *Journal of Sound and Vibration* 68 (1980) 427–436.
[29] K. Suzuki, H. Aida, S. Takahashi, Vibrations of curved bars perpendicular to their planes, *Bulletin of the Japan Society of Mechanical Engineers* 21 (1978) 162–173.
[30] S. Takahashi, K. Suzuki, Vibrations of elliptic arc bar perpendicular to its plane, *Bulletin of the Japan Society of Mechanical Engineers* 20 (1977) 1409–1416.
[31] M. Kawakami, T. Sakiyama, H. Matsuda, C. Morita, In-plane and out-of-plane free vibrations of curved beams with variable sections, *Journal of Sound and Vibration* 187 (1995) 381–401.
[32] K. Kang, C.W. Bert, A.G. Striz, Vibration analysis of shear deformable circular arches by the differential quadrature method, *Journal of Sound and Vibration* 181 (1995) 353–360.
[33] A.S. Gendy, A.F. Saleeb, Vibration analysis of coupled extensional/flexural/torsional modes of curved beams with arbitrary thin-walled sections, *Journal of Sound and Vibration* 174 (1994) 261–274.
[34] M.Y. Kim, N.I. Kim, B.C. Min, Analytical and numerical study on spatial free vibration of nonsymmetric thin-walled curved beams, *Journal of Sound and Vibration* 258 (2002) 595–618.
[35] A. Gjelsvik, *The Theory of Thin Walled Bars*, Wiley, New York, 1981.
[36] M.Y. Kim, S.B. Kim, N.I. Kim, Spatial stability of shear deformable curved beams with non-symmetric thin-walled sections. I: an improved stability formulation, *Journal of Engineering Mechanics*, under review.
[37] M.Y. Kim, N.I. Kim, H.T. Yun, Exact dynamic and static stiffness matrices of shear deformable thin-walled beam-columns, *Journal of Sound and Vibration* 267 (2003) 29–55.
[38] K.J. Bathe, *Finite Element Procedures*, Prentice-Hall, Englewood Cliffs, NJ, 1996.
[39] ABAQUS, *User's Manual. Vol. I and Vol. II. Ver. 5.2*, Hibbit, Karlsson, 1992.
[40] A.K. Noor, J.M. Peters, B.J. Min, Mixed finite element models for free vibrations of thin-walled beams, *Finite Elements in Analysis and Design* 5 (1989) 291–305.